

Algebraic correlation functions and anomalous diffusion in the Hamiltonian mean field model

Yoshiyuki Y Yamaguchi¹, Freddy Bouchet² and Thierry Dauxois³

¹ Department of Applied Mathematics and Physics, Graduate School of Informatics, Kyoto University, 606-8501, Kyoto, Japan

² Institut Non Linéaire de Nice, UMR-CNRS 6618, 1361 route des Lucioles, 06560 Valbonne, France

³ Laboratoire de Physique, ENS Lyon, CNRS, 46 Allée d'Italie, 69364 Lyon cedex 07, France

E-mail: yyama@amp.i.kyoto-u.ac.jp, Freddy.Bouchet@inln.cnrs.fr and Thierry.Dauxois@ens-lyon.fr

Received 6 October 2006

Accepted 9 January 2007

Published 30 January 2007

Online at stacks.iop.org/JSTAT/2007/P01020

[doi:10.1088/1742-5468/2007/01/P01020](https://doi.org/10.1088/1742-5468/2007/01/P01020)

Abstract. We numerically compute correlation functions of momenta and diffusion of angles with homogeneous initial conditions in the quasi-stationary states of the Hamiltonian mean field model. This is an example, in an N -body Hamiltonian system, of anomalous transport properties characterized by non-exponential relaxations and long-range temporal correlations. Kinetic theory predicts a striking transition between weak anomalous diffusion and strong anomalous diffusion. The numerical results are in excellent agreement with the quantitative predictions of the anomalous transport exponents. It is noteworthy that, at statistical equilibrium also, the system exhibits long-range temporal correlations: the correlation function is inversely proportional to time with a logarithmic correction instead of the usually expected exponential decay, leading to weak anomalous transport properties.

Keywords: stochastic particle dynamics (theory), slow dynamics and ageing (theory)

Contents

1. Introduction	2
2. Quantities of interest and numerical protocol	5
3. Power-law tails	6
3.1. Initial distribution	6
3.2. Stationarity and stability checks	6
3.3. Check of the theoretical prediction	7
4. Gaussian distribution	9
4.1. Initial distribution	9
4.2. Stationarity and stability checks	9
4.3. Check of the theoretical prediction	10
5. Summary	12
Acknowledgment	13
References	13

1. Introduction

Recently, new light was shed on long-range interacting systems [1]. The first reason is that a mathematical characterization [2] and the study of several simple models have completely clarified the inequivalence of ensembles that might exist between the microcanonical and the canonical ensembles [3, 4]. The second is the appearance of a very useful technique, namely the large deviation theory, for computing the microcanonical number of microstates and thus the associated microcanonical entropy [5]. The third is a classification of all possible situations of ensemble inequivalence [6]. The last, but not least, reason is the understanding that the broad spectrum of applications (self-gravitating [7] and Coulomb systems, vortices in two-dimensional fluid mechanics, wave-particle interaction, trapped charged particles, . . .) [1] should be considered simultaneously since significant advances were achieved independently in the different domains. However as usual in physics, the study of simple models is of particular interest not only for pedagogical properties, but also for testing ideas that might be derived analytically and verified numerically without very expensive simulations.

We consider here the Hamiltonian mean field (HMF) model, which is considered as the paradigmatic dynamical model for long-range interacting systems. This model [8]–[11] consists of N particles moving on the unit circle, and is described by the Hamiltonian

$$H = \frac{1}{2} \sum_{j=1}^N p_j^2 + \frac{1}{2N} \sum_{j=1}^N \sum_{k=1}^N [1 - \cos(\theta_j - \theta_k)], \quad (1)$$

where θ_j is the angle of the j th particle and p_j its conjugate momentum. Using a change of the time unit, the prefactor $1/N$ of the second term is added in order to get an extensive energy [5]. Thus, in the limit $N \rightarrow \infty$, the appropriate mean field scaling is obtained for the

statistical mechanics. Studies of the HMF model have been recently reinforced by the discovery of its link with the Colson–Bonifacio model for the single-pass free electron laser [5].

Within this model, a striking disagreement was reported between the canonical statistical mechanics predictions and time averages of constant energy molecular dynamics simulations [11, 12]. As the model has only a second-order phase transition [5] at the critical energy density $U_c = 3/4$, the possibility that the origin might lead to an inequivalence between canonical and microcanonical statistical mechanics can be excluded [6]. Moreover, recently, it has been shown unambiguously that the microcanonical entropy leads to the same predictions as the canonical free energy [5]. Very interesting results about the behaviour of such a system in contact with a thermal bath have however been recently reported [13, 14].

The origin of the apparent disagreement comes from a particularly slow dynamical evolution of this long-range system. Indeed, in Hamiltonian systems with long-range interactions, systems are sometimes trapped in quasi-stationary states (QSS) before going to equilibrium. Examples of such QSS were found in a one-dimensional self-gravitating system [15] and in the HMF model [16]. The trapping time diverges algebraically in the limit $N \rightarrow \infty$ and, hence, time averages disagree with canonical averages if the computing time is not long enough.

To understand the dynamics during such a long period, QSS were interpreted as stable stationary states of the Vlasov equation [17, 18] that can be derived from the Hamiltonian dynamics. The Vlasov equation, which governs the one-particle distribution function is indeed exact [19] in the limit $N \rightarrow \infty$, but only approximate for a finite system: finite size effects indeed drive the system from the Vlasov stable stationary state to the Boltzmann equilibrium. Recently, Caglioti and Rousset [20] proved, for a wide class of potentials which includes the HMF case, that N particles starting close to a Vlasov stable stationary state remain close to it for a timescale proportional to at least $N^{1/8}$. The result is consistent with numerical results which state that the lifetime of QSS scales like $N^{1.7}$ [16].

Using a kinetic approach which goes beyond the above Vlasov interpretation, the correlation function of momenta was recently derived [21, 22] with the following assumptions: (i) a finite but large enough number of particles, (ii) a homogeneous distribution of angles, and (iii) a system in a (quasi-)stationary state. As shown in [17, 18], the latter condition amounts to considering initial distributions of momenta $f_0(p)$ satisfying the inequality

$$1 + \frac{1}{2} \int_{-\infty}^{+\infty} \frac{f_0'(p)}{p} dp > 0. \quad (2)$$

This condition has been derived for the linear [23] and formal [17] stability of the distribution f_0 (see also [24] for another derivation). This condition defines a critical energy U_c^* which is, in general, different from the critical energy $U_c = 3/4$ where the second-order phase transition is located. However, as expected, the two values coincide for a Gaussian distribution $f_0(p)$. The above theory is expected to be valid in the time interval $1 \ll \tau \ll N$, where $\tau = t/N$ is the appropriate rescaled time.

Among the main predictions summarized in table 1, one might emphasize that distributions $f_0(p)$ with algebraic tails were proved to have a correlation function of momenta $C_p(\tau)$ with an algebraic decay in the long time regime. Striking algebraic

Table 1. Asymptotic forms of initial distributions $f_0(p)$, and theoretical predictions of correlation functions $C_p(\tau)$ and the diffusion $\sigma_\theta^2(\tau)$ in the long time regime. Asymptotic forms of the distribution and the predictions are assumed and predicted in the limits $|p| \rightarrow \infty$ and $\tau \rightarrow \infty$ respectively, where $\tau = t/N$ is a rescaled time. The exponent α is given as $\alpha = (\nu - 3)/(\nu + 2)$. See [22] for details.

Tails	$f_0(p)$	$C_p(\tau)$	$\sigma_\theta^2(\tau)$
Power law	$ p ^{-\nu}$	$\tau^{-\alpha}$	$\tau^{2-\alpha}$
Stretched exponential	$\exp(-\beta p ^\delta)$	$\frac{(\ln \tau)^{2/\delta}}{\tau}$	$\tau(\ln \tau)^{2/\delta+1}$

large time behaviours for momentum autocorrelations were first numerically observed in [12, 25]. In contrast, distributions with stretched exponential tails correspond to correlation functions inversely proportional to time with a logarithmic correction. It is also important to stress that Gaussian distributions, which correspond to $\delta = 2$ in the stretched exponential case, leads to a long time correlation of $\ln \tau/\tau$ instead of the usual exponential decay in the stable, supercritical energy regime $U > U_c^* = U_c$, although the initial distribution is at equilibrium. The origin of this unusual long time momentum correlation depends not on the centre part of the momentum distribution $f_0(p)$ but on its tails. One might understand this behaviour physically through the fact that particles located in these tails move almost freely, and hence yield long time correlations.

In these (quasi-)stationary states, the theoretical law for the diffusion of angles $\sigma_\theta^2(\tau)$ has also been derived. The predictions [22, 26] for the diffusion properties are listed in table 1. They clarify the highly debated disagreement between different numerical simulations reporting either anomalous [27] or normal [16] diffusion, in particular by delineating the time regime for which such anomalous behaviour should occur. We briefly recall that when the moment of order n of the distribution scales like $\tau^{n/2}$ at large time, such a transport is called *normal*. However, *anomalous* transport [28]–[30], where moments do not scale as in the diffusive case, were reported in some stochastic models, in continuous time random walks (Levy walks), and for systems with a lack of stationarity of the corresponding stochastic process [31]. When the distribution $f_0(p)$ is changed within the HMF model, a transition between weak anomalous diffusion (normal diffusion with logarithmic corrections) and strong anomalous diffusion is thus predicted. From the physical point of view, as particles with large momentum p fly very fast in comparison to the typical timescales of the fluctuations of the potential, they are subjected to a very weak diffusion and thus maintain their large momentum for a very long time. A thick distribution of waiting time with a large momentum explains the anomalous diffusion. From a mathematical point of view, these behaviours are linked to the non-exponential relaxation of the Fokker–Planck equation describing the diffusion of momenta, leading to long-range temporal correlations [22]. This mechanism is new in the context of kinetic theory. However, similar Fokker–Planck equations, with rapidly vanishing diffusion coefficients obtained from other physical mechanisms, have been studied in several frameworks [32]–[34].

The first purpose of this paper is to numerically check the theoretical predicted correlation functions for power-law tail and Gaussian distributions by using accurate

numerical simulations. The other is to clarify whether diffusion is normal or anomalous, which depends on the choice of the initial distribution $f_0(p)$.

The paper is organized as follows. Some useful quantities are introduced in section 2. In sections 3 and 4, we respectively focus on initial distributions with power-law and Gaussian tails. In each section, we first check the stationarity and the stability following the method developed in [17] and determine the time region of the QSS. We also study carefully the correlation function and the diffusion, comparing them with theoretical predictions. Finally, section 5 concludes the discussion.

2. Quantities of interest and numerical protocol

In order to check the stationarity and the stability of an initial distribution $f_0(p)$, we study the temporal evolutions of several macrovariables:

- The magnetization defined as the modulus M of the vector $\mathbf{M} = (M_x, M_y)$, where the two components are defined as $M_x = \langle \cos \theta \rangle_N$ and $M_y = \langle \sin \theta \rangle_N$. The bracket $\langle \cdot \rangle_N$ represents the average over all particles, for instance $\langle \cos \theta \rangle_N = (\sum_{j=1}^N \cos \theta_j)/N$. Note that the magnetization M is constant if the system is stable stationary.
- The moments of the one-body distribution function $f(\theta, p, t)$. As explained in detail in [17], the stationarity of the one-body distribution $f(\theta, p, t)$ implies the stationarity of the individual energy distribution $f_e(e, t)$, where $e = p^2/2 - M_x \cos \theta - M_y \sin \theta$. Moreover, the stationarity of $f_e(e, t)$ implies the stationarity of all moments $\mu_n = \langle e^n \rangle_N$. As the stationarity of the moment is a necessary condition for stability, vanishing derivatives $\dot{\mu}_n = d\mu_n/dt$, for $n = 1, 2$ and 3 , would suggest that the system is in a (quasi-)stationary state, while large derivatives clearly indicate a non-stationary state. In addition, stability is suggested if a state stays stationary for a long period.

While checking the stationarity and the stability, we identify a time region where the system is in the QSS, during which we observe the correlation function of momenta $C_p(\tau) = \langle p(\tau)p(0) \rangle_N$ and the diffusion of angles $\sigma_\theta^2(\tau) = \langle [\theta(\tau) - \theta(0)]^2 \rangle_N$. The latter quantity can be rewritten as follows:

$$\frac{\sigma_\theta^2(\tau)}{N^2} = \int_0^\tau d\tau_1 \int_0^\tau d\tau_2 \langle p(\tau_1)p(\tau_2) \rangle_N = 2 \int_0^\tau ds \int_0^{\tau-s} d\tau_2 \langle p(s+\tau_2)p(\tau_2) \rangle_N, \quad (3)$$

where the factor $1/N^2$ comes from the time rescaling $\tau = t/N$, while the new variable $s = \tau_1 - \tau_2$ was introduced to take advantage of the division of the square domain into two isoscale triangles corresponding to $s > 0$ and $s < 0$. In the (quasi-)stationary states, the integrand $\langle p(s+\tau_2)p(\tau_2) \rangle_N$ does not depend on τ_2 (the QSS evolve on a timescale much larger than N) and hence diffusion can be simplified [16] by using the correlation function as

$$\frac{\sigma_\theta^2(\tau)}{N^2} = 2 \int_0^\tau (\tau - s) C_p(s) ds. \quad (4)$$

We numerically performed the temporal evolution of the canonical equations of motion by using a fourth-order symplectic integrator [35, 36] with a time step $\Delta t = 0.2$ and a total momentum set to zero. The initial values of angles are randomly chosen from a homogeneous distribution; the magnetization M is hence of order $1/\sqrt{N}$. Omitting

this vanishing value of M , the energy density $U = K + (1 - M^2)/2$ where K is the kinetic energy density can thus be well approximated by the kinetic energy density K as $U = K + 1/2$. To characterize the simulations, the only remaining point is the initial distribution of momenta: in the following sections, as anticipated, we will carefully study distributions with power-law and Gaussian tails.

3. Power-law tails

3.1. Initial distribution

In this section, we consider the initial distribution

$$f_0(p) = \frac{A_\nu}{1 + |p/p_0|^\nu}, \quad (5)$$

whose power-law tails are characterized by the exponent ν . Unity, added in the denominator to avoid the divergence at the origin $p = 0$, does not affect either the asymptotic form, or the theoretical predictions. The parameter p_0 is directly determined by the kinetic energy density as $p_0 = (2K \sin(3\pi/\nu)/\sin(\pi/\nu))^{1/2}$, while the normalization factor is

$$A_\nu = \frac{\nu}{2\pi} \left(\frac{\sin^3(\pi/\nu)}{2K \sin(3\pi/\nu)} \right)^{1/2}. \quad (6)$$

From the stability criterion (2), one gets that this initial state is Vlasov stable when the kinetic energy density satisfies the condition

$$K > \frac{1}{4} \frac{\sin(\pi/\nu)}{\sin(3\pi/\nu)}. \quad (7)$$

One thus gets a dynamical critical energy $U_c^* = 0.75, 0.625$ and $0.60355\dots$ for $\nu = 4, 6$ and 8 respectively. In the rest of this section, we set the exponent ν to 8 .

3.2. Stationarity and stability checks

Let us numerically check the stationarity and the stability of these states; in particular, it will clarify the time region of existence of the QSS. Figure 1 presents the temporal evolution of M and $\dot{\mu}_n$ ($n = 1, 2, 3$) for the unstable ($U = 0.6 < U_c^*$) and stable ($U = 0.7 > U_c^*$) cases. In both cases, the magnetization M eventually goes toward the equilibrium value M_{eq} , indicated by horizontal lines. The three quantities $\dot{\mu}_n$ have vanishing small fluctuations around zero except during the time interval $0.0005 < \tau < 0.003$ for the unstable case. In the unstable case, the system is first in an unstable stationary state ($\tau < 0.0005$), before becoming non-stationary ($0.0005 < \tau < 0.003$) and finally reaches stable stationary states ($\tau > 0.003$). On the other hand, in the stable case, the stable stationarity holds throughout the computed time.

In the stable case, the magnetization M stays around zero before taking off around $\tau = 20$ to reach the equilibrium value M_{eq} . The fluctuation level of $\dot{\mu}_n$ increases around the take-off time $\tau = 20$, but the increase does not imply any non-stationarity of the system, since the fluctuation level is 10 times smaller than the corresponding one in the non-stationary time region of the unstable case. The non-zero magnetization might be at

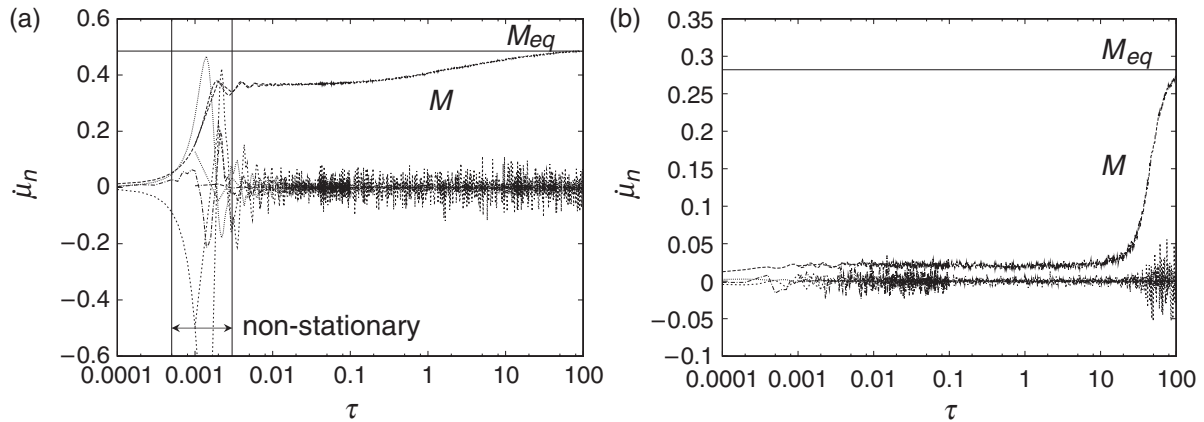


Figure 1. Stationarity check for initial distributions with power-law tails. Note the logarithmic scale for the rescaled time $\tau = t/N$. Panel (a) presents the unstable case $U = 0.6$ while panel (b) shows the stable one $U = 0.7$. The three curves $\dot{\mu}_n$ ($n = 1, 2, 3$) are reported in both panels. Their vertical scales are multiplied by 100 for graphical purposes. Curves and horizontal lines indicated by symbols M and M_{eq} represent respectively temporal evolutions of the magnetization and its equilibrium value. All numerical curves are obtained by averaging 20 different numerical simulations for $N = 10^4$.

the origin of the fluctuations being larger than in the zero-magnetization cases, since the former has a phase and an individual energy e which depends not only on the modulus M but also on the phase.

3.3. Check of the theoretical prediction

For the stable case ($U = 0.7$), we perform numerical computations for $N = 10^3, 10^4, 2 \times 10^4$ and 5×10^4 , and average over 20, 20, 10 and 5 sample orbits respectively. Temporal evolutions of magnetization M are shown in figure 2(a), and M takes off toward the equilibrium value M_{eq} around $\tau_2 = 1, 20$ and 50 for $N = 10^3, 10^4$ and 2×10^4 respectively. The take-off time defines the end of the applicable time region of the theory since the homogeneous assumption (ii) breaks. Note that no take-off time appears in the case $N = 5 \times 10^4$, within the computed time interval.

The theory predicts (see table 1 for $\nu = 8$) that the correlation function decays algebraically with the exponent $-1/2$, i.e. $C_p(\tau) \sim \tau^{-1/2}$, up to the take-off time τ_2 . According to figure 2(b), the theoretical prediction agrees well with numerical computations in the intermediate time region $\tau_1 < \tau < \tau_2$, where $\tau_1 = 2$ for any value N . This is expected since, on the one hand, the short time region $\tau < \tau_1$ is out of the time domain of application since the theory gives asymptotic estimates. The time τ_1 is marked as a long vertical line in figure 2(b) to clearly indicate the start of the applicable time domain. Although the quantity $\tau_s \simeq 0.005$ is not derived theoretically, the straight lines with the slope $-1/2$ in figure 2(b), representing $(\tau/\tau_s)^{-1/2}$, emphasize the agreement of the predicted exponent.

Introducing the expression for the correlation function in relation (4) leads to the law $\sigma_\theta^2(\tau) \sim \tau^{3/2}$: figure 2(c), in which the four curves for the four different values of

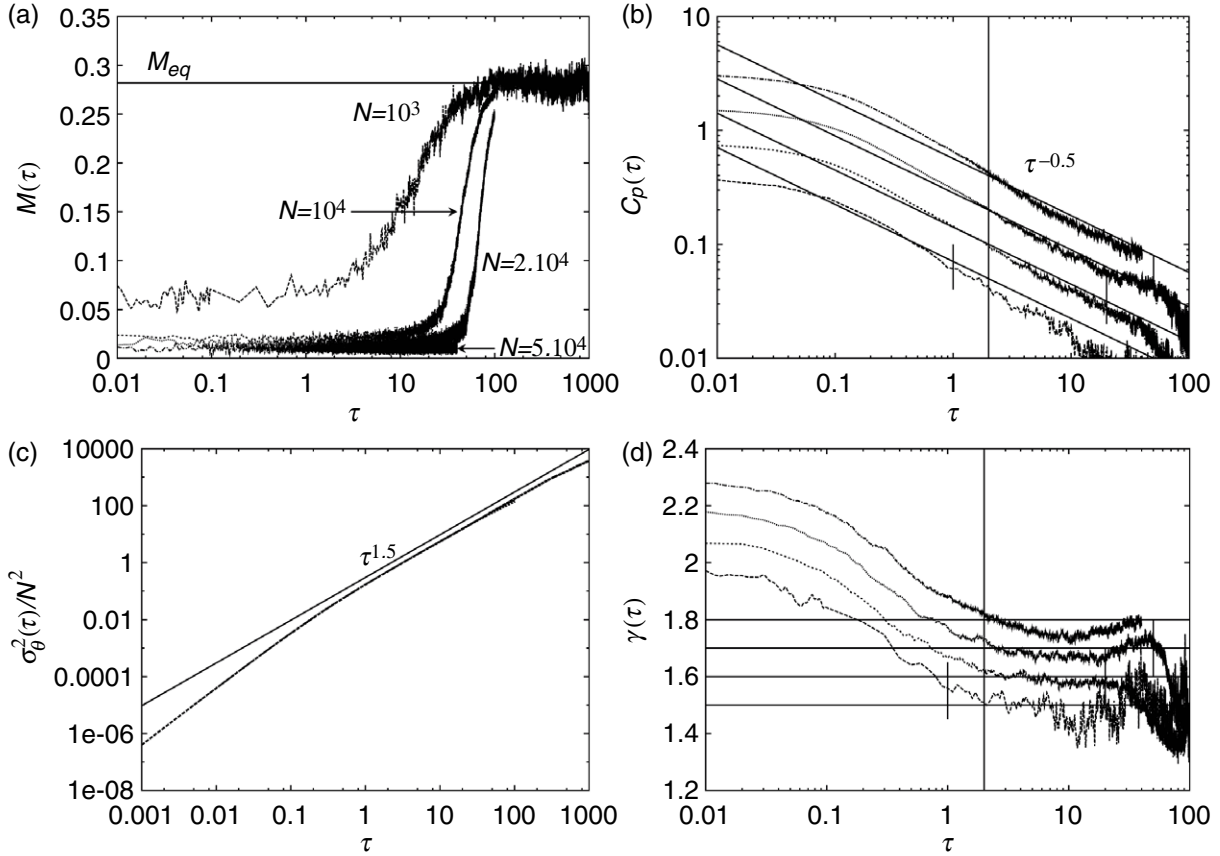


Figure 2. Check of the theoretical prediction for stable initial distributions with power-law tails, for the case $U = 0.7$. Points are numerically obtained by averaging 20, 20, 10 and 5 realizations for $N = 10^3, 10^4, 2 \times 10^4$ and 5×10^4 respectively. Panel (a) shows the temporal evolution of the magnetization with the timescale $\tau = t/N$. The take-off times of M are estimated as $\tau_2 = 1, 20$ and 50 for $N = 10^3, 10^4$ and 2×10^4 respectively, and the τ_2 are marked in panels (b) and (d). No take-off for $N = 5 \times 10^4$ is observed in this computing time. The horizontal line represents the equilibrium value of M . In panel (b), four curves represent the correlation functions of momenta, while the straight lines with the slope $-1/2$ represent the theoretical prediction. The curves and the lines are multiplied from the original vertical values by 2, 4 and 8 for $N = 10^4, 2 \times 10^4$ and 5×10^4 for graphical purposes. The vertical line indicates $\tau_1 = 2$ from which the valid time region of the theory starts. Similarly, panel (c) presents the diffusion of angles, while the straight line with the slope $3/2$ is theoretically predicted. The four curves for the four different values of N are reported and almost collapse. Finally, panel (d) shows the temporal evolution of the instantaneous exponent γ , defined in equation (8), and γ stays around the theoretically predicted value $3/2$ in the time region $\tau_1 < \tau < \tau_2$. The values 0.1, 0.2 and 0.3 are added in vertical values for $N = 10^4, 2 \times 10^4$ and 5×10^4 respectively for graphical purposes.

N almost collapse, attests also to the validity of this prediction in the intermediate time region $\tau_1 < \tau < \tau_2$. It is possible to confirm more precisely that the diffusion exponent is $3/2$ by introducing the instantaneous exponent γ [37] defined as

$$\gamma = \frac{d \ln \sigma_\theta^2(\tau)}{d \ln \tau} = \frac{1}{\sigma_\theta^2(\tau)} \frac{d\sigma_\theta^2(\tau)}{d \ln \tau}. \quad (8)$$

The instantaneous exponent γ , shown in figure 2(d), goes down and once crosses $3/2$. However, γ comes back and stays around $3/2$ in the time interval $\tau_1 < \tau < \tau_2$. The above result confirms therefore unambiguously that the diffusion is anomalous, namely superdiffusive, in the intermediate QSS time interval as predicted by the theory [22].

The temporal evolution of γ was also recently discussed by Antoniazzi *et al* [38], and was shown to monotonically decrease toward 1. The difference has two different origins: first, Antoniazzi *et al* considered non-homogeneous initial distributions of angles, which are out of the applicable range of the theory tested here; second, they considered a water-bag initial distribution of momenta, which does not have tails initially, although tails develop of course as soon as the time is slightly positive. As the theory states that the asymptotic law for diffusion is determined by the tails of the initial distribution of momenta, there is no contradiction in the temporal evolution of γ being different. A similar remark applied with the out-of-equilibrium initial distribution discussed by Moyano and Anteneodo [37].

For the power-law tail initial distributions, the theoretical predictions are essentially good, but not exact. We first note that the increase of N does not affect either the correlation function, or the diffusion, at least for $10^4 \leq N \leq 5 \times 10^4$ (the case $N = 10^3$ has been excluded since no validity time region $\tau_1 < \tau < \tau_2$ appears). In the numerical results, the slope of the diffusion γ is not 1.5 but belongs to $[1.44, 1.48]$. The relative discrepancy is thus at most of 4%. There are two possibilities for understanding this small discrepancy: (a) the lack of the samples, and (b) the lack of stationarity which is the assumption (iii) of the theory. We will discuss the origin of these discrepancies at the end of the next section.

4. Gaussian distribution

4.1. Initial distribution

In this section, we consider the Gaussian initial distribution

$$f_0(p) = \frac{1}{\sqrt{2\pi T}} e^{-p^2/2T}, \quad (9)$$

where the initial temperature T is determined from the energy density as $T = 2K = 2U - 1$. The dynamical critical energy of this Gaussian distribution coincides with the critical energy of the second-order phase transition $U_c = 3/4$. As the distribution of angles is homogeneous, the system is therefore at equilibrium for any supercritical energy $U > U_c$.

4.2. Stationarity and stability checks

The stationarity and stability are checked as in section 3.2 by considering temporal evolutions of magnetization and the derivatives of moments μ_n shown in figure 3. The

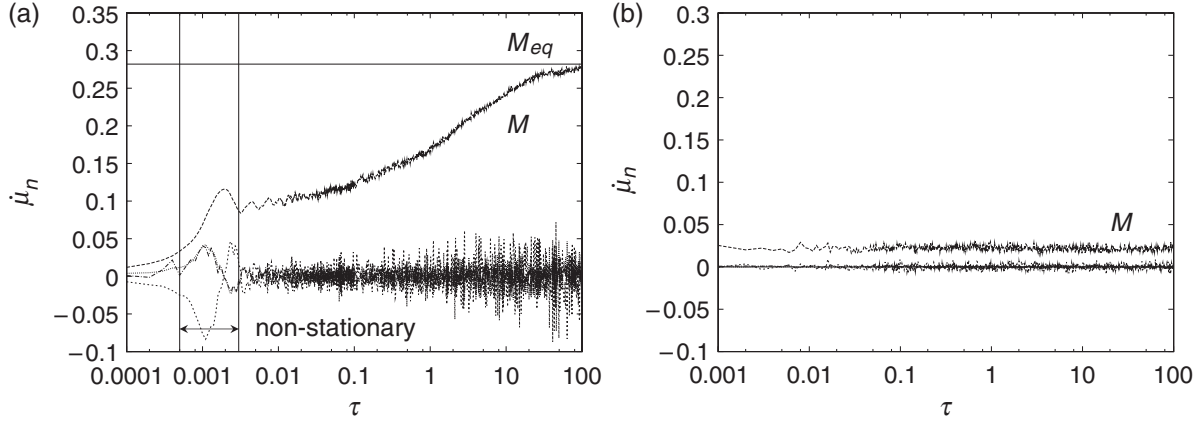


Figure 3. Stationarity check for Gaussian initial distributions with $N = 10^4$. Note the logarithmic scale for the rescaled time $\tau = t/N$. Panel (a) presents the unstable case $U = 0.7$ while panel (b) shows the stable one $U = 0.8$. The three curves $\hat{\mu}_n$ ($n = 1, 2, 3$) are reported in both panels. Their vertical scales are multiplied by 100 for graphical purposes. Curves indicated by the symbol M represent the temporal evolutions of the magnetization. In panel (a), the horizontal line indicated by M_{eq} represents the equilibrium value, while in panel (b), the equilibrium value is zero. All numerical curves are obtained by averaging 20 different numerical simulations.

scenario of relaxation of this initial distribution with power-law tails is very similar. In the unstable case ($U = 0.7 < U_c$), the system reaches stable stationary states after experiencing unstable stationary and non-stationary states. In the stable case ($U = 0.8 > U_c$), the state is stable stationary in the whole time domain since it is initially at equilibrium.

4.3. Check of the theoretical prediction

Let us focus on the stable case $U = 0.8$ with $N = 10^4$. The correlation function obtained numerically, and shown in figure 4(a), is in good agreement with the theoretical prediction $(\ln \tau)/\tau$ in the long time region $\tau > \tau_1 = 1$ if we accept the second scaling of time as $\tau \rightarrow \tau/\tau_s$ with $\tau_s = 0.2$. As already mentioned in section 3.3, the second scaling is not provided by the theory, while the asymptotic theoretical estimate is out of the range of applicability in the short time domain $\tau < \tau_1$. We would like also to stress that the logarithmic correction makes the prediction more precise rather than a simple algebraic decay $1/\tau$.

The correlation function can thus be approximated as

$$C_p(\tau) = \begin{cases} C_p(0), & \text{if } \tau < \tau_1, \\ \frac{c\tau_s}{\tau} \ln \frac{\tau}{\tau_s}, & \text{if } \tau > \tau_1, \end{cases} \quad (10)$$

where the short time value has to be $C_p(0) = \langle p^2(0) \rangle_N = 2K = 0.6$, while $c = 0.85$ is obtained by a fitting procedure. This approximation of the correlation function and the

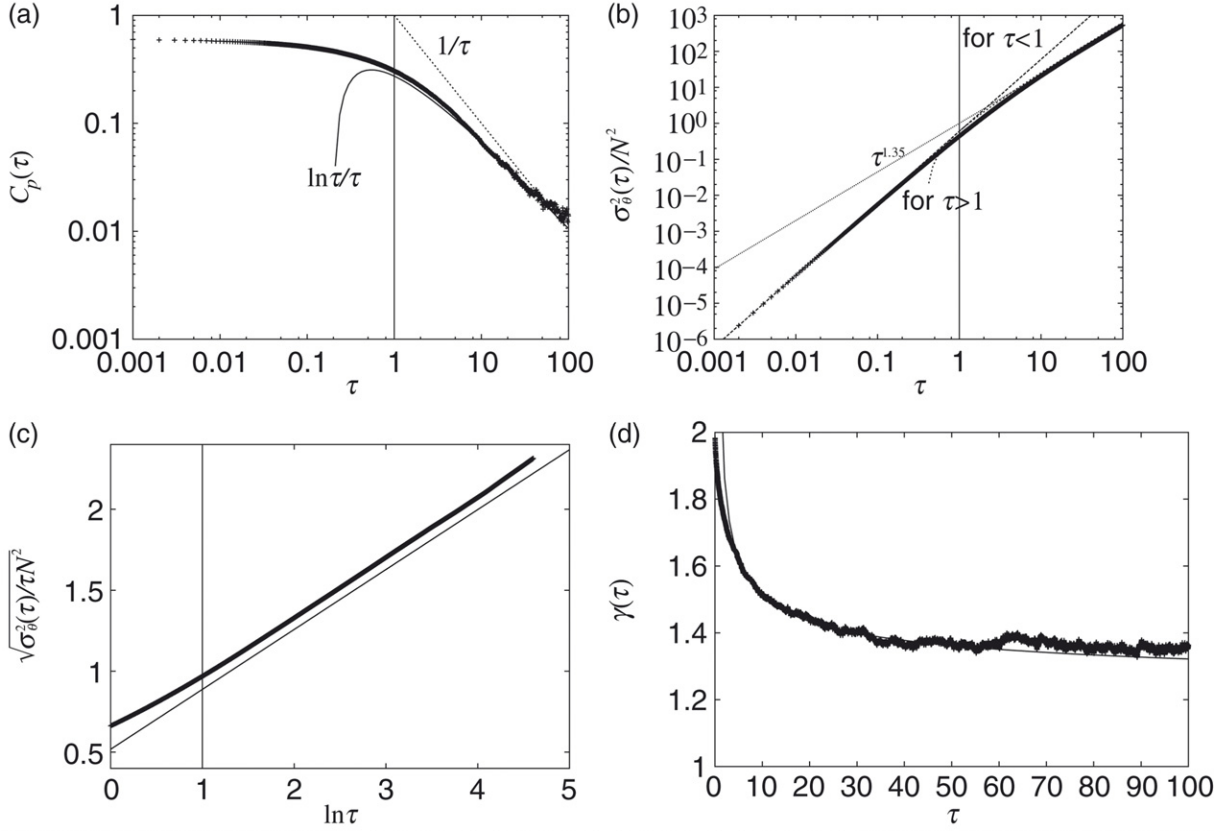


Figure 4. Check of the theoretical prediction for Gaussian stable initial distributions for the case $U = 0.8$ with $N = 10^4$. Points are numerically obtained by averaging 20 realizations. In panel (a), the symbols show the correlation function of momenta. The theoretical prediction, $\ln\tau/\tau$, is a better approximation than the simpler law $1/\tau$. Panel (b) presents the diffusion of angles. Although the diffusion is normal, the straight line $\tau^{1.35}$ wrongly suggests that it is not. See the text for explanations and details. Panel (c) shows the quantity $\sqrt{\sigma_\theta^2(\tau)/(\tau N^2)}$ as a function of $\ln\tau$, to confirm the logarithmic correction of the diffusion. The straight line is a guide for the eyes. Finally, panel (d) presents the temporal evolution of the instantaneous exponent γ . The dashed line corresponds to relation (12).

relation (4) leads to the following expression for the diffusion:

$$\frac{\sigma_\theta^2(\tau)}{N^2} = \begin{cases} C_p(0)\tau^2, & \text{if } \tau < \tau_1, \\ 2C_p(0) \left(\tau_1\tau - \frac{\tau_1^2}{2} \right) + c\tau_s\tau \left[\left(\ln \frac{\tau}{\tau_s} \right)^2 - \left(\ln \frac{\tau_1}{\tau_s} \right)^2 \right] \\ - 2c\tau_s \left[\tau \left(\ln \frac{\tau}{\tau_s} - 1 \right) - \tau_1 \left(\ln \frac{\tau_1}{\tau_s} - 1 \right) \right], & \text{if } \tau > \tau_1. \end{cases} \quad (11)$$

Figure 4(b) presents the diffusion obtained numerically. Both curves indicating the short and long time regions show a very good agreement. The diffusion seems anomalous

with an exponent 1.35 in the long time region. Similarly, the instantaneous exponent γ seems to converge toward 1.35 as shown by figure 4(d). However, these observations are not accurate, and only due to a long transient, induced by the logarithmic correction. Diffusion is essentially proportional to the time τ , and hence must be normal in the asymptotic time region. Expression (11) provides the asymptotic form of the instantaneous exponent

$$\gamma = 1 + \frac{2}{\ln(\tau/\tau_s)}. \quad (12)$$

This prediction is in good agreement with numerical results as attested by figure 4(d). In the limit of $\tau \rightarrow \infty$, the exponent γ goes logarithmically toward unity, and we therefore conclude that diffusion is normal although a long transient time is necessary to observe it. This is an excellent illustration of the difficulty of getting reliable numerical estimates for the diffusion exponent. Such a case explains *a posteriori* the reason for the previous disagreement [16, 27].

As predicted by table 1, the logarithmic correction of the correlation function yields a logarithmic correction of the diffusion, so that its asymptotic form should be $\sigma_\theta^2(\tau)/N^2 \sim \tau(\ln \tau)^2$. Figure 4(c) confirms this prediction, plotting $\sqrt{\sigma_\theta^2(\tau)/(\tau N^2)}$ as a function of $\ln \tau$: one gets a linear behaviour in the long time region $\tau > 1$. We thus have confirmed the existence of weak anomalous diffusion, i.e. normal diffusion with logarithmic corrections.

Let us return to the origin of discrepancies for α and γ , discussed at the end of the previous section for the power-law tails. It seems natural to exclude the possibility (a), lack of samples, since the same number of orbits, 20, has been used in the case $N = 10^4$, for both the power-law tails and the Gaussians, while the latter case agrees extremely well with the theoretical predictions, even including the logarithmic correction. This excellent agreement comes from the absence of any breaking of theoretical assumptions, since the state is at equilibrium and stationary accordingly. Consequently, we can consider that the possibility (b), lack of stationarity, explains the discrepancies of α and γ for power-law tails.

5. Summary

We have numerically confirmed the theoretical predictions proposed in [22] for initial distributions with power-law or Gaussian tails: the correlation function and diffusion are in good agreement with numerical results. Diffusion is indeed *anomalous superdiffusion* in the case of power-law tails, while it is *normal* for the Gaussian case. In the latter case, the system is at equilibrium, but the diffusion exponent shows a logarithmically slow convergence to unity due to a logarithmic correction of the correlation function. This long transient time for observing normal diffusion, even for Gaussian distribution and at equilibrium, suggests that one should be very careful in deciding whether diffusion is anomalous or not [39]–[41].

For the power-law tail initial distribution, the numerically obtained exponent of diffusion is slightly different from the theoretical prediction (a few per cent). As discussed above, this discrepancy comes from the breaking of the stationary assumption. The state is only approximately stationary, explaining why the theoretical predictions are not exact but only approximate. We stress that in the limit of large N , these states become

stationary because their live times diverge much faster than N . For the Gaussian initial distribution, the state is in equilibrium from the start, and stationary even with finite N : hence the theoretical predictions agree extremely well with numerical results.

In addition, the above numerical computations clarify two new points: (i) the time region where the theory is applicable, (ii) the second time scaling to fit the correlation function and the diffusion. Both might depend on the degrees of freedom, but the latter, (ii), appears to be not the case for the power-law tails. Obtaining the dependence for the Gaussian is future work.

Finally, let us remark that the scenario of the relaxation described in [17, 18] is confirmed even for initial distributions with power-law tails: this had never been tested previously. The scenario claims that the system with long-range interactions experiences first a violent relaxation, before the so-called collisional relaxation which drives the system toward Boltzmann's equilibrium. In the simulations reported here, non-stationary and stable stationary states correspond respectively to the violent and the collisional relaxations. One might also remark that distributions with power-law tails induce quasi-stationary states above the dynamical critical energy, while not being q -distributions [42]. The latter might be a sufficient condition of QSS, but is definitely not a necessary condition. To conclude let us remark that if the results discussed here concern the simple HMF model, we should mention that it is believed to be general for long-range interacting systems [43, 44].

Acknowledgment

YYY has been supported by the Ministry of Education, Science, Sports and Culture, Grant-in-Aid for Young Scientists (B), 16740223, 2006.

References

- [1] Dauxois T, Ruffo S, Arimondo E and Wilkens M (ed) 2002 *Dynamics and Thermodynamics of Systems with Long Range Interactions (Springer Lecture Notes in Physics vol 602)* (Berlin: Springer)
- [2] Ellis R S, Haven K and Turkington B, 2000 *J. Stat. Phys.* **101** 999
- [3] Barré J, Mukamel D and Ruffo S, 2001 *Phys. Rev. Lett.* **87** 030601
- [4] Ellis R S, Touchette H and Turkington B, 2004 *Physica A* **335** 518
- [5] Barré J, Bouchet F, Dauxois T and Ruffo S, 2005 *J. Stat. Phys.* **119** 677
- [6] Bouchet F and Barré J, 2005 *J. Stat. Phys.* **118** 1073
- [7] Chavanis P H, Sommeria J and Robert R, 1996 *Astrophys. J.* **471** 385
- [8] Zaslavsky G M, Shabanov V F, Aleksandrov K S and Aleksandrov I P, 1977 *Sov. Phys. JETP* **45** 315
- [9] Konishi T and Kaneko K, 1992 *J. Phys. A: Math. Gen.* **25** 6283
- [10] Pichon C, 1994 *PhD Thesis* Cambridge
- [11] Antoni M and Ruffo S, 1995 *Phys. Rev. E* **52** 2361
- [12] Latora V, Rapisarda A and Tsallis C, 2001 *Phys. Rev. E* **64** 056134
- [13] Baldovin F and Orlandini E, 2006 *Phys. Rev. Lett.* **96** 240602
- [14] Baldovin F and Orlandini E, 2006 *Phys. Rev. Lett.* **97** 100601
- [15] Tsuchiya T, Gouda N and Konishi T, 1996 *Phys. Rev. E* **53** 2210
- [16] Yamaguchi Y Y, 2003 *Phys. Rev. E* **68** 066210
- [17] Yamaguchi Y Y, Barré J, Bouchet F, Dauxois T and Ruffo S, 2004 *Physica A* **337** 36
- [18] Barré J, Bouchet F, Dauxois T, Ruffo S and Yamaguchi Y Y, 2006 *Physica A* **365** 177
- [19] Braun W and Hepp K, 1977 *Commun. Math. Phys.* **56** 101
- [20] Caglioti E and Rousset F, *Long time estimates in the mean field limit*, 2004 *Preprint* HYKE 2004-157, <http://www.hyke.org/preprint/2004/15/157.pdf>
- [21] Bouchet F and Dauxois T, 2005 *J. Phys.: Conf. Ser.* **7** 34
- [22] Bouchet F and Dauxois T, 2005 *Phys. Rev. E* **72** 045103(R)
- [23] Inagaki S and Konishi T, 1993 *Publ. Astron. Soc. Japan* **45** 733

- [24] Chavanis P H, Vatteville J and Bouchet F, 2005 *Eur. Phys. J. B* **46** 61
- [25] Pluchino A, Latora V and Rapisarda A, 2004 *Phys. Rev. E* **69** 056113
- [26] Bouchet F, 2004 *Phys. Rev. E* **70** 036113
- [27] Latora V, Rapisarda A and Ruffo S, 1999 *Phys. Rev. Lett.* **83** 2104
- [28] Bouchaud J P and Georges A, 1990 *Phys. Rep.* **195** 127
- [29] Majda A J and Kramer P R, 1999 *Phys. Rep.* **314** 238
- [30] Castiglione P, Mazzino A, Muratore-Ginanneschi P and Vulpiani A, 1999 *Physica D* **134** 75
- [31] Bouchet F, Cecconi F and Vulpiani A, 2004 *Phys. Rev. Lett.* **92** 040601
- [32] Farago J, 2000 *Europhys. Lett.* **52** 379
- [33] Lillo F *et al*, 2002 Preprint [cond-mat/0203442](https://arxiv.org/abs/cond-mat/0203442)
- [34] Lutz E, 2004 *Phys. Rev. Lett.* **93** 190602
- [35] Yoshida H, 1990 *Phys. Lett. A* **150** 262
- [36] Yoshida H, 1993 *Celest. Mech. Dyn. Astron.* **56** 27
- [37] Moyano L G and Anteneodo C, 2006 *Phys. Rev. E* **74** 021118
- [38] Antoniazzi A, Fanelli D, Barré J, Chavanis P-H, Dauxois T and Ruffo S, 2007 *Phys. Rev. E* **75** 011112
- [39] Pluchino A, Latora V and Rapisarda A, 2004 *Physica A* **340** 187
- [40] Pluchino A, Latora V and Rapisarda A, 2004 *Physica D* **193** 315
- [41] Zanette D and Montemurro M, 2003 *Phys. Rev. E* **67** 031105
- [42] Tsallis C, 1988 *J. Stat. Phys.* **52** 479
- [43] Chavanis P H and Lemou M, 2005 *Phys. Rev. E* **72** 061106
- [44] Chavanis P H, 2006 *Eur. Phys. J. B* **52** 61